

# A 3D Array High-Gain Vivaldi Antenna Design

Hongyang Xu\*, Haisheng Song

School of Chemistry and Chemical Engineering, Northwest Normal University, Lanzhou 730070, China

\*Corresponding author: Hongyang Xu (E-mail: 13259770734@163.com)

---

**Abstract:** This article designs a 3D array high-gain Vivaldi antenna suitable for K-band. First, by adding a positive trapezoidal dielectric structure to the radiation port of the original Vivaldi antenna unit, the purpose is to increase the gain of the Vivaldi antenna unit. The Vivaldi antenna unit was simulated and analyzed through HFSS software to obtain a new Vivaldi antenna unit with a frequency band width of 20GHz-26.4GHz and a gain of 10.8dB. Wider bandwidth, improved gain performance and enhanced directionality of the Vivaldi antenna unit compared to the original antenna. A 4-cell antenna array with a 3D structure is designed in order to be suitable for smaller planar size operating environments, and the antenna structure is further analyzed by...In this paper, the power division feed network conforming to this array is designed and the performance of this 2×2 antenna array is investigated, and the simulation results show that this array has good bandwidth and radiation performance, strong directionality, and almost no offset angle in the E-plane.

**Keywords:** 3D array; Vivaldi antenna; Pilot; High gain; Power division feed network; Directionality; Bandwidth.

---

## 1. Introduction

The rapid development of radar technology, the emergence of miniaturized, low-cost radar, so that the application of radar is more extensive, vehicle collision avoidance radar came into being. In the process of automobile driving, collision avoidance radar can pre-judge whether the surrounding vehicles and obstacles will have an impact on the automobile driving, and then through the issuance of warnings to draw the attention of the driver to the possible dangers that may occur, and if the driver is too late to react, it can also be a temporary substitute for the driver to make a deceleration to avoid or emergency braking and other safety operations to avoid accidents.

Currently, the two frequency bands used internationally for on-board radar are 24 GHz and 77 GHz. Of these, 24 GHz is used for short-range radar, where the Vivaldi antenna has good radiation characteristics and a wide bandwidth. In 1979, Gibson first proposed a tapered chipped slot antenna using exponentially tapering curves, known as a conventional antenna, which belongs to the category of tapering, non-periodic, end-shooting traveling-wave antennas, in which electromagnetic waves are radiated from the narrower gap end to the wider open end by means of an exponentially tapering slit structure. In order to improve the performance of the antenna, loading of metamaterials on top of conventional structures, introduction of slit structures, loading of dielectric lenses, etc. are usually used. The Vivaldi conventional antenna unit proposed in literature has a gain of 6.3 dB at an operating frequency of 24 GHz and its operating bandwidth is 23-27 GHz. Literature proposes to add an inverted trapezoidal guide to the radiating port of the heeled Vivaldi antenna, and the gain of the prototype heeled Vivaldi antenna is 10 dB at 24 GHz operating frequency, and the gain rises to 12.8 dB after the addition of the guide, however, literature only improves the gain of the heeled Vivaldi antenna, and no research has been carried out in the aspect of the conventional Vivaldi antenna. Literature proposes to load a rectangular slot on a conventional Vivaldi antenna with a bandwidth of 2-4 GHz operating band and a triangular pilot at the radiating port, the antenna has a gain of 6.7 dB at an operating frequency of

3 GHz, which is a total gain improvement of 1.8 dB compared to the conventional Vivaldi antenna.

In this paper, a new high-gain Vivaldi antenna unit at 24 GHz is proposed to add a positive trapezoidal structure at the radiating port of a conventional Vivaldi antenna with a bandwidth of 20 GHz-26.4 GHz, and the maximum gain is about 10.8 dB at the operating frequency of 24 GHz. Compared to literature there is a great improvement in terms of gain and bandwidth. Compared to literature this paper applies the idea of a pilot to a conventional Vivaldi antenna with appropriate structural changes. Compared to literature where this paper improves the gain by 1 dB when only the pilot is loaded, literature improves it by only 0.8 dB. And this paper proposes a 2×2 3D structure of the array and designs a common feed network to match with it, so that its array increases 4.2dB compared to the cell gain and the bandwidth is 5.9GHz, which meets the design and requirements.

In this paper, a 3D 4-cell 2×2 array antenna operating at 24 GHz frequency has been designed by investigating the array, feed, etc. As in literature to design a 1 × 4 linear array of Vivaldi antenna units, this design compared to its linear array 1 × 4 array, greatly reducing the size required for the array plane, and other performance has been improved for the design of Vivaldi antenna arrays to provide a new way of thinking.

## 2. 24GHz Vivaldi Antenna Unit Design

### 2.1. Calculation of the original antenna unit and its dimensions

The schematic of the original Vivaldi antenna structure is shown in Figure 1 below.

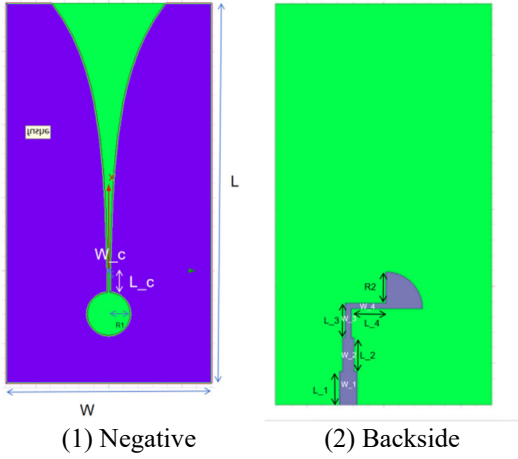


Figure 1. Traditional Vivaldi antenna structure

### (1) Slotted line structure

Vivaldi antenna is a traveling wave antenna with end-shooting characteristics, according to the radiation principle of Vivaldi antenna, it can be known that the antenna starts to radiate electromagnetic waves only when the slot line end opening is larger than  $1/2$  wavelength, so when the frequency is increased to the width of slot line end opening is larger than  $1/2$ , the antenna starts to radiate electromagnetic waves outward, so the width of the slot line end opening decides the low-frequency characteristics of the antenna, and when the frequency is continued to increase, the antenna is not able to radiate efficiently when the width of the antenna's starting end is larger than two times the wavelength, therefore, the width of slot line starting end decides the antenna's high-frequency characteristics[4].

Knowing the width of the openings at the beginning and end of the exponential tapering groove line, the exponential tapering groove line can be sized using the formula for exponential tapering groove lines.

Vivaldi index gradient groove line formula

$$y = \pm(C_1 e^{rx} + C_2) \quad (1)$$

$$C_1 = \frac{y_2 - y_1}{e^{rx_2} - e^{rx_1}} \quad (2)$$

$$C_2 = \frac{y_1 e^{rx_2} - y_2 e^{rx_1}}{e^{rx_2} - e^{rx_1}} \quad (3)$$

Where,  $(x_1, y_1)$ ,  $(x_2, y_2)$  are the coordinates of the start point and end point,  $r$  is the curvature of the slot line, which determines the degree of curvature of the slot line, when  $r$  is larger, the more curved the exponential asymptotic curve is, the lower the low frequency cutoff frequency is, and the better the antenna's low-frequency characteristics are, and vice versa.

### (2) Radial-slot line structure

Vivaldi antenna by the microstrip line to the slot line feed, according to the Vivaldi antenna principle, this form of balun disadvantage is narrow bandwidth, so in order to further broaden the bandwidth of the balun, the lower end of the microstrip line to extend the branch section into a fan-shaped short cut-off line structure, so as to make the microstrip line in the wider band to maintain an open-circuit state. The extended branch section at the lower end of the slotline is converted into a circular resonant cavity structure, which ensures that the end of the slotline remains short-circuited over a wide frequency band[1]. The diameter  $D$  of the circular

resonant cavity is  $1/4$  of the slotline waveguide wavelength, and the radius of the short fan-shaped section is  $1/4$  of the microstrip line waveguide wavelength.

### (3) $1/4$ Multi-section impedance matching network

By the formula of microstrip line and slot line and the relationship between microstrip line characteristic impedance and slot line characteristic impedance as shown in the following equation.

$$Z_s = N^2 * Z_m \quad (4)$$

Where,  $N$  is a conversion factor of size.

$$N = \cos(2\pi ud/\lambda_0) - \cot(q) \sin(2\pi ud/\lambda_0) \quad (5)$$

$$q = 2\pi ud/\lambda_0 + \tan^{-1} \quad (6)$$

$$U = \sqrt{\epsilon_r - (\lambda_0/\lambda_s)^2} \quad (7)$$

$$V = \sqrt{(\lambda_0/\lambda_s)^2 - 1} \quad (8)$$

According to the theory of small reflections, this paper uses a multi-section Chebyshev impedance converter with reflection coefficients, as in the following equation:  $\Gamma(\theta) = 2e^{-Nj\theta} [\Gamma_0 \cos N\theta + \Gamma_1 \cos(N-2)\theta + \dots + \Gamma_n \cos(N-2n)\theta + \dots] = Ae^{-jN\theta} T_N(\sec\theta_m \cos\theta)$ .

When designing a Chebyshev multinode impedance converter, the coefficients of the polynomial ( $|A|$ ) are first determined based on the maximum reflection coefficient ( $\Gamma_m$ ) allowed in the passband.

$$\Gamma_m = |A| \quad (9)$$

The number of matching sections  $N$  is found according to the following equation:

$$\theta_m = \frac{\pi(2 - \Delta f/f_0)}{4} \quad (10)$$

$$\sec\theta_m = \cosh * \left[ \frac{1}{N} \cosh^{-1} \left( \left| \frac{\ln Z_L/Z_0}{2T_m} \right| \right) \right] \quad (11)$$

In the formula,  $Z_L$  represents the load impedance, and  $Z_0$  represents the input impedance, i.e.  $50\Omega$ .

Find the impedance of each section in turn based on the following equation:

$$\Gamma_n = \frac{1}{2} \ln \frac{Z_{n+1}}{Z_n} \quad (12)$$

In this paper,  $N = 4$  is obtained, so the physical dimensions of the conventional Vivaldi antenna are shown in Table 1, with length in mm.

Table 1. Vivaldi antenna unit dimensions

| L      | W      | R1  | R2   | H      | L c | L 1    | W 1    |
|--------|--------|-----|------|--------|-----|--------|--------|
| 26.017 | 14.05  | 1.5 | 2.39 | 0.5008 | 1.5 | 2.1625 | 1.152  |
| W 2    | L 3    | W 3 | L 4  | W 4    | r   | W c    | L 2    |
| 0.7512 | 2.2275 | 0.4 | 2.25 | 0.39   | 0.2 | 0.2    | 2.1925 |

## 2.2. High gain 24 GHz Vivaldi antenna unit design and simulation

A forward trapezoidal deflector is added to the radiating port of the original Vivaldi antenna unit, as shown in Figure 2. The addition of the pilot structure is known to enhance the

surface current at the radiating port and increase the gain of the Vivaldi antenna unit. In this paper, the addition of a positive trapezoidal dielectric plate at the radiating port can limit the radiation direction of the surface current at the port to the antenna, thus enhancing the gain of the antenna unit. Using the parameter optimization function of the HFSS software, the size parameter of  $W_t$  was determined to be 0.39 mm, and its physical dimensions are shown in Table II in mm.

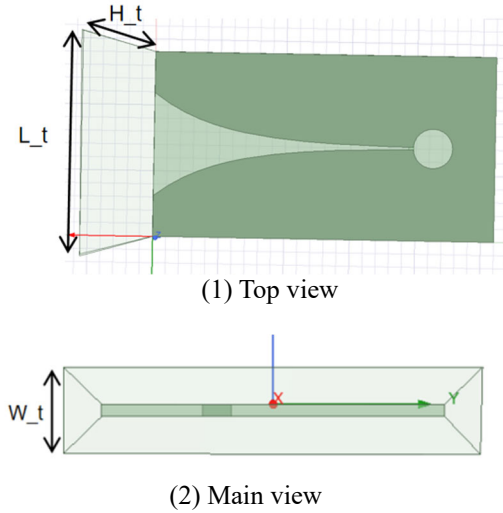


Figure 2. New Vivaldi antenna unit

Table 2. Dimensions of trapezoidal media structures

| $\theta$   | $L_t$ | $W_t$  | $H_t$ |
|------------|-------|--------|-------|
| $15^\circ$ | 17.16 | 3.5008 | 5.6   |

Using HFSS software, a  $50 \Omega$  collector port is added at the excitation source, and the surface current simulation analysis of the original Vivaldi antenna cell and the new Vivaldi antenna cell are carried out respectively, and it can be found that the currents of the radiating cell are mainly distributed in

the vicinity of the tapering slot, which is in accordance with the principle. Surface current simulation distribution is obtained Figure 3. From Figure 3, it can be found that the current strength of the original Vivaldi antenna (b) at the radiating port is relatively weak. It can be found that the current strength of the new Vivaldi antenna (a) at the radiating port is significantly enhanced after the addition of the trapezoidal dielectric structure, so it can be concluded that after the addition of the trapezoidal dielectric structure, the surface currents are concentrated at the radiating port of the antenna, which enhances the antenna's radiating characteristics and improves the antenna unit's gain.

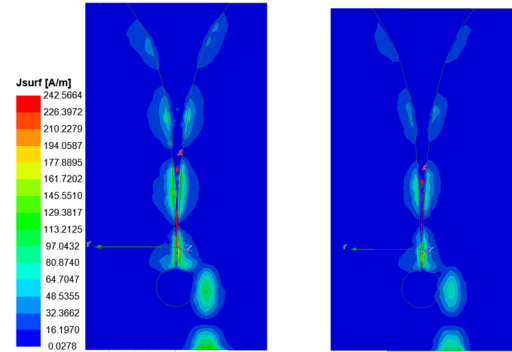


Figure 3. Comparison of surface current simulation

Comparing with the S-parameters and gain characteristics of the original Vivaldi antenna unit, the S-parameter simulation results are obtained as shown in Fig. 4, and it can be observed that the return loss of the new Vivaldi antenna is less than -10dB in the bandwidth of 20GHz-26.4GHz, and even less than -15dB in the bandwidth of 21.5GHz-24.9GHz, and reaches -26.2dB in the frequency of 23.3 GHz, it reaches -26.2 dB; compared with the original Vivaldi antenna, the bandwidth is wider, with a bandwidth of 6.4 GHz, and the return loss at 24 GHz is lower.

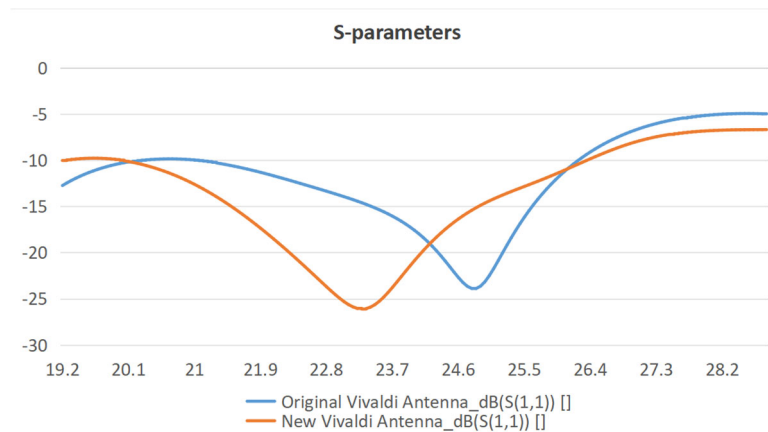


Figure 4. S-parameter simulation results of the novel Vivaldi antenna

The simulation results of the gain direction diagram of the new Vivaldi antenna and the original Vivaldi antenna at a frequency of 24 GHz are shown in Figure 5. From Figure 5(a), it can be seen that after adding the positive trapezoidal dielectric structure, the gain of the new Vivaldi antenna reaches about 10.8 dB higher than that of the original Vivaldi antenna at a frequency of 24 GHz, which is about 1 dB higher

than that of the original Vivaldi antenna, and it can be clearly seen that the sub-flap of the Vivaldi antenna is reduced. And through the directional map of the antenna in Figure 5(b), it is clearly observed that the beam width of the new antenna unit is narrower, indicating that the new Vivaldi antenna unit is more directional.

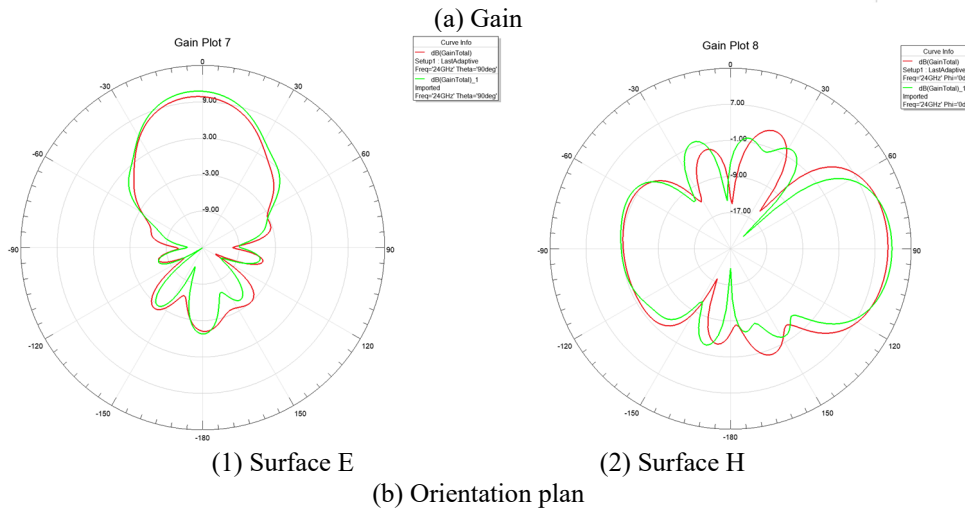
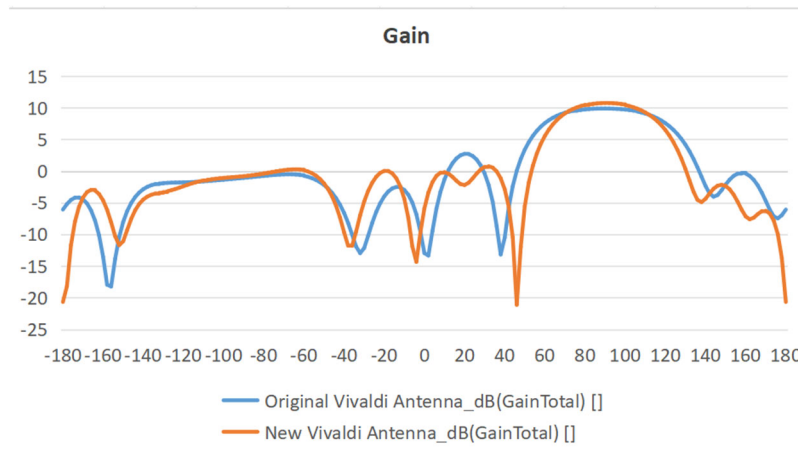


Figure 5. Gain and Direction Graph

### 3. Power Divider Feeder Network Design and Simulation

First, according to the designed array and unit, because the feeding part of the Vivaldi antenna is fed by microstrip feeding and it is a top and bottom structured array, so in this paper, the power divider adopts the microstrip-coaxial-microstrip feeding structure, which utilizes the transmission characteristics of coaxial and microstrip lines to realize the signal transmission of the array.

From the point of view of the circuit analysis, firstly the characteristic impedance of the feed part of the antenna unit is 50 ohms, to realize a feed network with a characteristic impedance of 50-50 ohms, and secondly there are four units in the array, so it is necessary to make a one-part-two-repeat-two power divider, whose equivalent circuit diagram is shown below in figure 6.

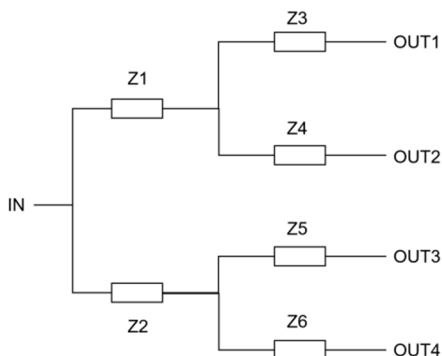


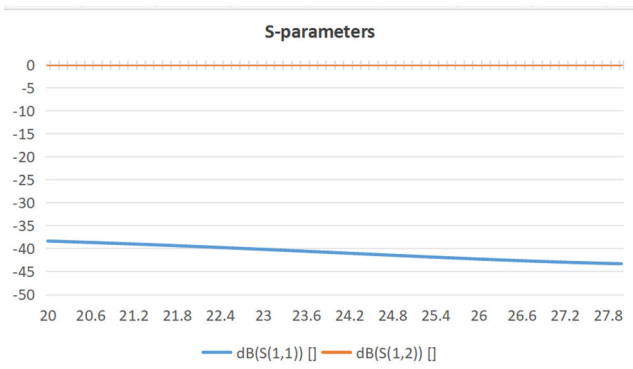
Figure 6. Schematic diagram of equivalent circuit

Because  $Z_0 = 50 \Omega$ , according to the Wilkinson power divider principle, this gives  $Z_1 = Z_2 = 100 \Omega$ . In order to realize the impedance matching of the transmission line,  $Z_1, Z_2$  is processed through the quarter wavelength in impedance transformation principle, which makes  $Z'_1 = Z'_2 = 50 \Omega$ , Consequently,  $Z_3 = Z_4 = Z_5 = Z_6 = 100 \Omega$ . In order to realize impedance matching between the power divider and the antenna, the principle of quadrature wavelength transformation is used in the same way so that  $Z'_3 = Z'_4 = Z'_5 = Z'_6 = 50 \Omega$ .

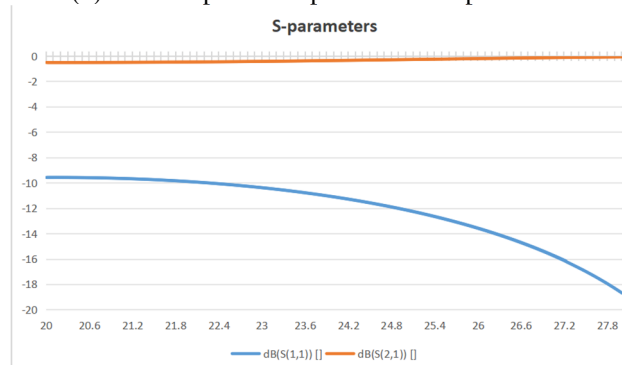
Considering that the whole array is three-dimensional, it is necessary to use coaxial lines to connect the upper and lower microstrip power dividers, as shown in Figure 8, and in this paper, we consider two structures of microstrip-coaxial connection.

The upper and lower microstrip lines have the same characteristic impedance where they are connected to the coaxial line. The upper microstrip line has a characteristic impedance of  $50 \Omega$ , and the lower microstrip line has a characteristic impedance of  $100 \Omega$ . Impedance matching is performed using coaxial lines

So the two methods were simulated and tested and the results are shown in Figure 7 below.



(1) Same impedance up and down S-parameter



(2) Different S-parameters for upper and lower impedance  
**Figure 7.** Test results of S-parameters for two cases

From the above figure, we can find that (1) the test results are better, (1) the  $S_{11}$  is bigger, indicating that only a weak signal is reflected back, (1) the  $S_{12}$  tends to be close to 0, indicating that the input is as much as the output, and there is basically no loss in the transmission process. The test result of (2), on the other hand, indicates that there is some loss of signal on the coaxial line.

Therefore, the microstrip-coaxial structure in this paper adopts the way of (1), so the design of the power divider needs to fully consider the structure of (1), according to the formula of the coaxial line, this paper adopts the coaxial line with an inner column radius of 0.05 mm and an outer column radius of 0.5925 mm, connecting the microstrip line to the coaxial line with the coaxial line with a high height of 14.5 mm, and its common denominator feeder network is shown in Figure 8.

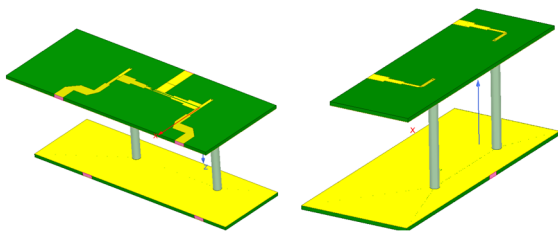


**Figure 8.** Fractional feeder network

By optimizing some parameters of the microstrip line and coaxial line, the simulation results of the return loss profile of the final power division feeder network are shown in Fig. 9 below.

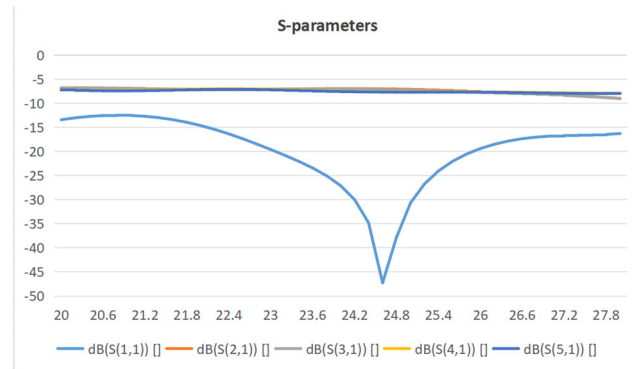


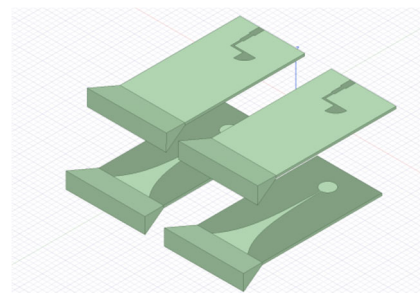
**Figure 9.** Return loss of a power-divided feeder network

The power division feeder network designed in this paper is fed in a one-in-four manner, with 1 as the input port and 2, 3, 4, and 5 as the output ports, and it can be seen that  $S_{11}$  is less than -10dB in the frequency band of 20-28GHz, and reaches -48dB at 24.6GHz, and below -28dB at 24GHz, which indicates that there is only a tiny amount of signal reflection,  $S_{12}$ ,  $S_{13}$ ,  $S_{14}$ , and  $S_{15}$  of this feeder network, are all greater than -7dB in the frequency band of 20-28GHz. The above simulation results show that in the operating band, the power divider, divides the input signal at port 1 nearly uniformly among the four output ports 2, 3, 4, and 5, and there is basically no signal reflected back. The bandwidth of the power division feed network designed in this paper is applicable to the new Vivaldi antenna designed in this paper and satisfies the design requirements.

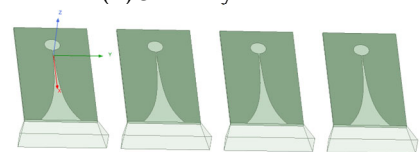
## 4. Array Design

### 4.1. Array structure

From the design point of view, in order to reduce the plane size of the array, so the design of a double-layer 3D  $2 \times 2$  arrays, but by the mutual coupling between the units, so the characteristics of their arrays and units work alone when the characteristics of the difference is very large, so the further study of the antenna unit and in the performance of the array, the simulation study, the structure of the structure as shown in Figure 10 (1).



(1) 3D array structure



(2) Linear array structure

**Figure 10.** Array structure

The structure of the array is that the spacing between the upper two cells is 5.77 mm, the spacing between the lower two cells is 7.34 mm, and the spacing between the upper and lower cells is 13.5 mm, which realizes the 3D array and

occupies a planar area of  $42.7 \times 34.35$ . The planar area of a  $1 \times 4$  linear array is  $75 \times 31.6$ , so the structure greatly reduces the planar area required by a 4-cell linear antenna array (e.g., Figure 10(2)). The structure greatly reduces the plane area required for a 4-cell linear antenna array (as in Figure 10(2)).

## 4.2. Array Simulation

Synthesizing the above articles, we obtain the array antenna shown in Fig. 11 below, with slight variations in performance due to the effects of mutual coupling between the units, and losses on each device.

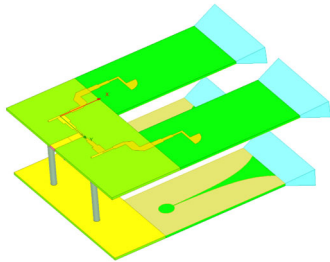


Figure 11. Schematic of array antenna

In this paper, the 3D array is composed of  $2 \times 2$  arrays, which greatly reduces the plane area required for the 4-unit array, and at the center frequency of 24 GHz, Figure 12 shows the simulation results of the 3D array without common feed network and the linear array, which shows that the gain of the 3D array with reactive power division feed network is 16 dB, and the main flap beamwidth is about  $26^\circ$ , which is basically the same as that of the linear array of  $1 \times 4$ , and the main flap beamwidth is narrower than that of the linear array. It is basically the same, and the main flap beamwidth is narrower compared to the linear array, which indicates that the 3D array is more directional, and the bandwidth of the 3D array is 6.4 GHz compared to the linear array, which is wider.

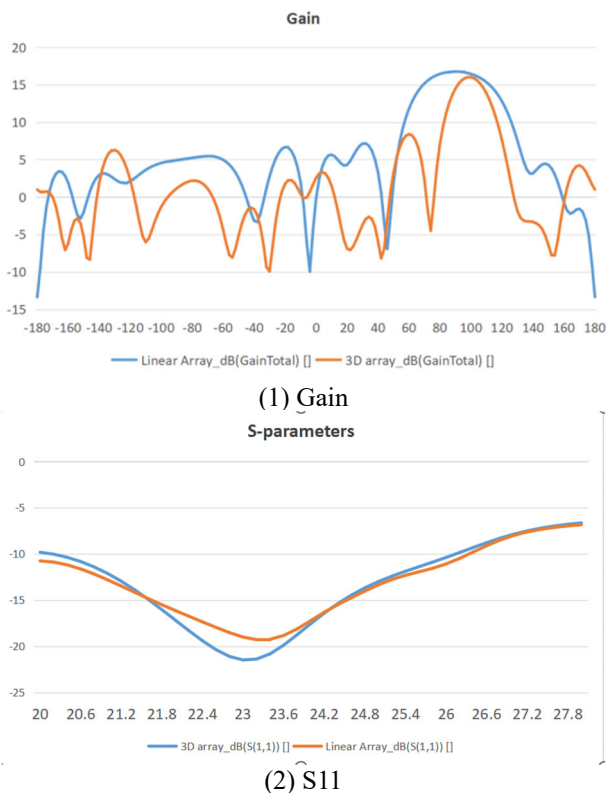


Figure 12. Comparison of simulation results between 3D array and linear array of power division free feeder network

At the center frequency of 24 GHz, Figure 13 shows the simulation comparison results of the final 3D array Vivaldi antenna designed in this paper, and it can be seen that the gain of this 3D array antenna is about -15 dB, and the main flap beamwidth is about  $23^\circ$ , compared with the array antenna without common feed network, the gain is slightly decreased, mainly due to the increase of the power divider circuit, the internal loss increase, and some parameters. The design is slightly flawed, resulting in a weak reflection of the signal in the transmission process can not achieve the ideal transmission, but the results are basically in line with the principle. By comparing the data, it can be seen that its directionality is stronger, and reduce the sub-flap, after adding the power division feed network, it can be obviously found to improve the antenna's E-plane offset angle so that it reaches  $90^\circ$ , although the bandwidth basically remains unchanged, but in the 24GHz operating frequency, the return loss number reaches -43dB, to reach the lowest return loss, and to meet the design requirements.

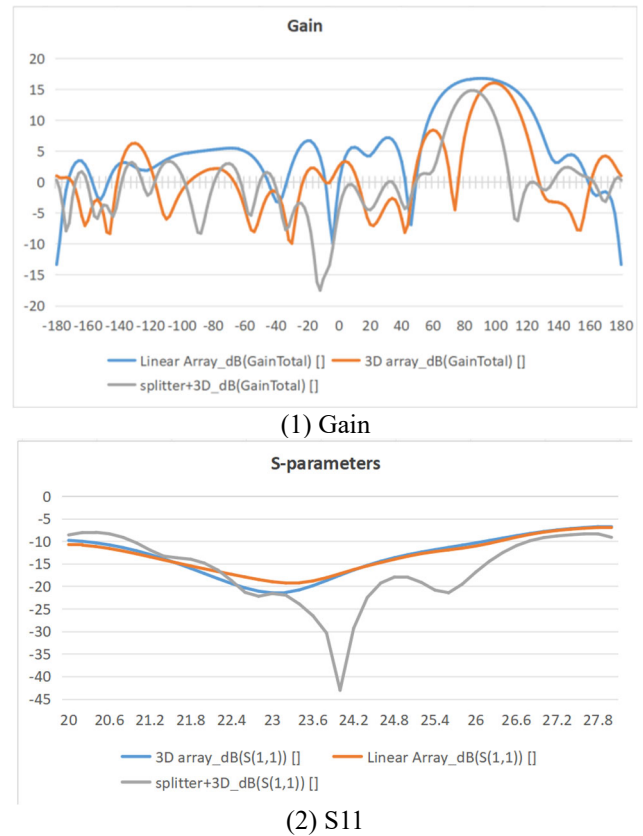


Figure 13. Comparison results of simulation of power-division-containing feeder networks

Figure 13 (2) shows the simulation comparison results of the return loss S11 of the array antenna containing the power-division feeding network, and the bandwidth of the array antenna designed in this paper is less than -10 dB within 21-26.9 GHz, and it is even less than -15 dB within the bandwidth of 22 GHz-26 GHz, and it reaches -43 dB at the frequency of 24 GHz.

## 5. Conclusion

In this paper, a new ultra-wideband high-gain Vivaldi antenna unit with a gain of 10.8 dB at an operating frequency of 24 GHz is designed. The antenna is based on the original Vivaldi antenna, and a positive trapezoidal dielectric structure plate is added to its radiating port to enhance the antenna's

surface currents at the radiating port, which not only reduces the sub-flap of the antenna unit, but also strengthens the antenna's radiating characteristics and Directionality. The return loss of the antenna is less than -10dB in the bandwidth of 20GHz-26.4GHz, and it has good characteristic impedance. In this paper, on top of the antenna unit, a 4-cell 3D antenna array operating at 24 GHz is also designed, and its matched common feed network is investigated. The array greatly reduces the plane area required for a typical 4-cell linear antenna array and has stronger directionality, with a gain of 15 dB at an operating frequency of 24 GHz, and the return loss of the antenna is less than -10 dB in a bandwidth of 21 GHz-26.9 GHz, and improves the gain peak offset angle of the E-plane directional map of the array antenna.

## Acknowledgment

This work is supported by the National Natural Science Foundation of China (11747030) and the Science and Technology Program of Gansu Province (20JR10RA080).

## References

- [1] Jian Ze. Study of SISL-based antennas and their arrays [D]. Chengdu: University of Electronic Science and Technology of China, 2018.
- [2] IkechukwuK. Ukaegbu. Parametric Analysis and Bandwidth Optimisation of HybridLinear-exponential Tapered Slot Vivaldi Antennas [A]. Loughborough Antennas & Propagation Conference (LAPC 2017) [C]. Loughborough: IET, 2017.
- [3] WANG Long. Design of Van Atta Array Based on Vivaldi Antenna [J]. *Microwave Journal*, 2019, 35(7): 62-65.
- [4] Rong Tan. Research on Miniaturization and Low-Scattering Technologies of Ultra-Wide band Dual-Polarized Vivaldi Antennas. D.A Thesis Submitted to Southeast University, Nanjing. DIO Number:10.27014/d.cnki.gdnau, 2021.001918.
- [5] DuHe. Vivaldi antennas and their engineering [D]. Xi'an: Xidian University, 2020.
- [6] Zhengbiao Wang. Bandwidth- and Gain-Enhanced Vivaldi Antenna Array Fed by Non-uniform T-junction Power Divider for Radio Astronomy Application [A]. 2018 12th International Symposium on Antennas, Propagation and EM Theory (ISAPE) [C]. Hangzhou, China: IEEE, 2018.
- [7] GengXin. Miniaturized airborne antenna design [D]. Xi'an: Xi'an University, 2021.
- [8] ShiXinRong. Ultra-wideband Vivaldi antenna unit and array design [J]. *Journal of Chinese Academy of Electronic Science*, 2020, 11: 1065-1069.
- [9] ChenJun. An ultra-wide band high-gain-to-heel Vivaldi antenna [J]. *Journal of Nanjing University of Information Engineering*, 2021, 13(4): 461-466.
- [10] Wang Mengmeng. S-band high gain Vivaldi antenna design [J]. *Microwave Journal*, 2020, 36: 105-108.
- [11] Wang Li Li. Liu Qing. Ultra-wide band Vivaldi antenna with low RCS for radar stealth equipment [J]. *Journal of electronic measurement and instrumentation*, 2022, 36(3): 122-129.